

Supporting Information

S1. This section presents details of the diffusion models employed in this study which were fitted to the normalised signal. Since the b_0 measurements have a significant diffusion weighting due to the imaging gradients of the STEAM sequence, especially for longer mixing time, this effect is accounted for in the signal equation:

$$\hat{S} = \frac{S_b}{S_{b_0}},$$

where \hat{S} is the measured normalized signal and S_b is the normalized diffusion signal for a given nominal b-value. The effective b matrices and signal models which include the effect of the imaging gradients and crushers are calculated based on the equations derived in (1).

Models for ex-vivo data		
Ball	Equation:	$S_b = \exp(-bD)$, b is calculated according to equation 10 and 11 in []
	Fitted parameters (1):	D
	Parameter range:	$0 < D < 3 \mu\text{m}^2/\text{ms}$
Kurtosis	Equation:	$S_b = \exp(-bD + \frac{1}{6} kD^2b^2)$
	Fitted parameters (2):	D and k
	Parameter range:	$0 < D < 3 \mu\text{m}^2/\text{ms}, 0 < k < 3$
Tensor	Equation:	$S_b = \exp(-\langle \mathbf{b}, \mathbf{D} \rangle)$, <, > denotes the inner product between the \mathbf{b} and \mathbf{D} tensors
	Fitted parameters (6):	$D_{ }, D_{\perp 1}, D_{\perp 2}, \theta, \varphi, \psi$ (tensor eigenvalues, and angles in spherical coordinates)
	Parameter range:	$0 < D_{\perp 2} < D_{\perp 1} < D_{ } < 3 \mu\text{m}^2/\text{ms}$
BallBall	Equation:	$S_b = f \exp(-bD_1) + (1 - f)\exp(-bD_2)$
	Fitted parameters (3):	f, D_1, D_2
	Parameter range:	$0 < D_2 < D_1 < 3 \mu\text{m}^2/\text{ms}; 0 < f < 1$
ZeppelinBall	Equation:	$S_b = f \exp(-\langle \mathbf{b}, \mathbf{D} \rangle) + (1 - f)\exp(-bD_2)$, \mathbf{D} is a cylindrically symmetric diffusion tensor with $D_{ } > D_{\perp 1} = D_{\perp 2}$
	Fitted parameters (6):	f, $D_{ }, D_{\perp 1}, D_2, \theta, \varphi$
	Parameter range:	$0 < D_{\perp 1} < D_{ } < 3 \mu\text{m}^2/\text{ms}; 0 < f < 1; D_2 < D_{ }$

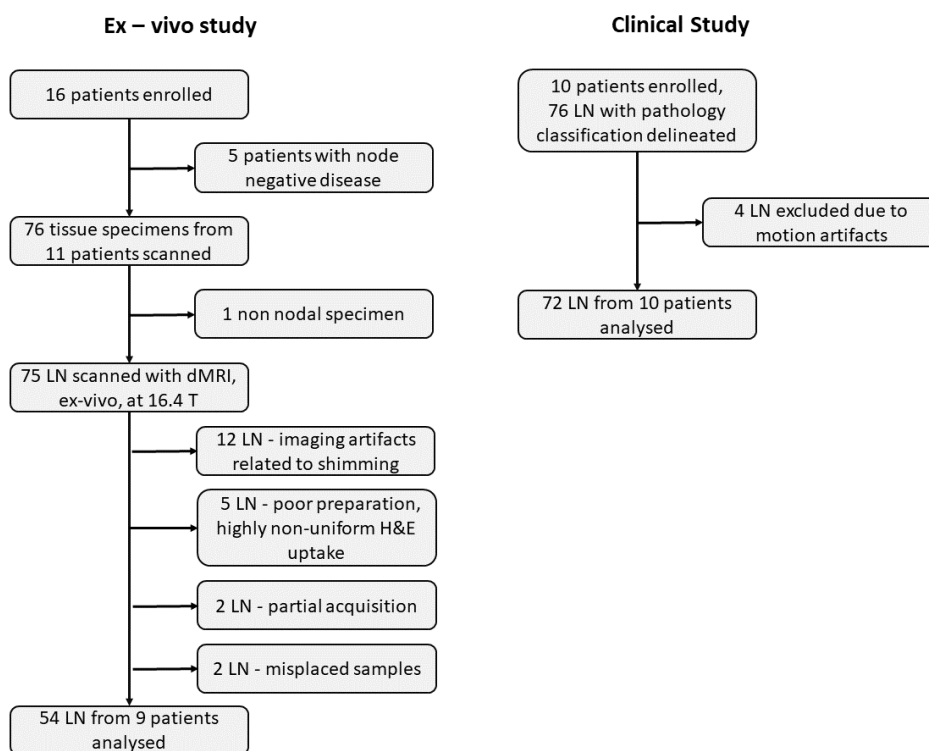
BallSphere	Equation:	$S_b = f S_{sphere} + (1 - f) \exp(-bD_2)$ $S_{sphere} = \exp\left(-\frac{\gamma^2}{D^2} \sum_{k=0}^{\infty} \frac{B_k I_k}{\lambda_k^2}\right), B_k = \frac{2(R/\mu_k)^2}{\mu_k^2 - 2}, \lambda_k = \left(\frac{\mu_k}{R}\right)^2$ <p>where R is the radius, μ_k is the k^{th} root of the equation $\mu J'_{3/2}(\mu) - \frac{1}{2} J_{3/2}(\mu) = 0$, and $J_{3/2}$ is a Bessel function of the first kind. I_k is a factor which depends on the diffusion STEAM sequence parameters and is given in equations 16-22 in (1).</p>
	Fitted parameters (3):	f, D, R
	Parameter range:	$0 < D < 3 \mu\text{m}^2/\text{ms}$; $0 < f < 1$; $0 < R < 30 \mu\text{m}$; $D_2 = D$
ZeppelinSphere	Equation:	$S_b = f S_{sphere} + (1 - f) \exp(-\langle \mathbf{b}, \mathbf{D} \rangle)$ <p>\mathbf{D} is a cylindrically symmetric diffusion tensor with $D_{\parallel} > D_{\perp 1} = D_{\perp 2}$ S_{sphere} is given above</p>
	Fitted parameters (6):	f, D, D_{\perp} , R, θ , φ
	Parameter range:	$0 < D_{\perp} < D < 3 \mu\text{m}^2/\text{ms}$; $0 < f < 1$; $0 < R < 30 \mu\text{m}$; $D = D_{\parallel}$
BallFiniteCylinder	Equation:	$S_b = f S_{FiniteCyl} + (1 - f) \exp(-bD_2)$ <p>$S_{FiniteCyl} = S_{Cyl} S_{plane}$, where S_{Cyl} and S_{plane} have the same form as S_{sphere} with different expressions for B_k and λ_k.</p> <p>For cylinder of radius R: $B_k = \frac{2(R/\mu_k)^2}{\mu_k^2 - 1}$, $\lambda_k = \left(\frac{\mu_k}{R}\right)^2$, where μ_k is the k^{th} root of the equation $J'_1(\mu) = 0$, and J_1 is a Bessel function of the first kind.</p> <p>For parallel planes separated by distance L: $B_k = \frac{8 L^2}{(2k-1)^4 \pi^4}$ $\lambda_k = \frac{\pi^2 (2k-1)^2}{L^2}$</p>
	Fitted parameters (6):	f, D, R, L, θ , φ
	Parameter range:	$0 < D < 3 \mu\text{m}^2/\text{ms}$; $0 < f < 1$; $0 < R < 30 \mu\text{m}$; $R < L < 100 \mu\text{m}$, $D = D_2$

Supporting Information Table S1 Description of the diffusion models fitted to the pre-clinical ex-vivo data including model name, equation, number of fitted parameters and the range of parameter values.

Models for clinical data		
Ball	Equation:	$S_b = \exp(-bD)$,
	Fitted parameters (1):	D
	Parameter range:	$0 < D < 3 \mu\text{m}^2/\text{ms}$
Kurtosis	Equation:	$S_b = \exp(-bD + \frac{1}{6} kD^2b^2)$
	Fitted parameters (2):	D and k
	Parameter range:	$0 < D < 3 \mu\text{m}^2/\text{ms}, 0 < k < 3$
IVIM	Equation:	$S_b = f \exp(-bD^*) + (1 - f)\exp(-bD)$
	Fitted parameters (3):	f, D*, D
	Parameter range:	$0 < D < 3 \mu\text{m}^2/\text{ms}; 3 < D^* < 30 \mu\text{m}^2/\text{ms}; 0 < f < 1$
IVIM Kurtosis	Equation:	$S_b = f \exp(-bD^*) + (1 - f)\exp(-bD + \frac{1}{6} kD^2b^2)$
	Fitted parameters (4):	f, D*, D, k
	Parameter range:	$0 < D < 3 \mu\text{m}^2/\text{ms}; 3 < D^* < 30 \mu\text{m}^2/\text{ms}; 0 < f < 1; 0 < k < 3$

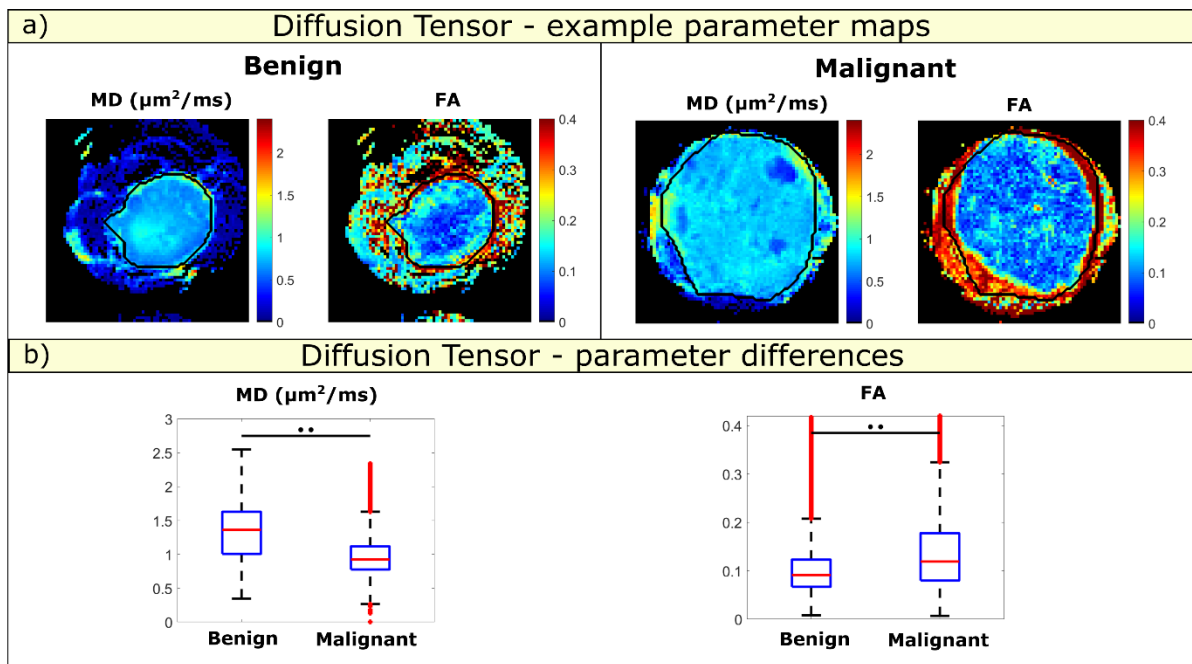
Supporting Information Table S2 Description of the diffusion models fitted to the clinical data including model name, equation, number of fitted parameters and the range of parameter values.

S2. This section details the criteria for excluding lymph nodes from the ex-vivo and in-vivo analysis.



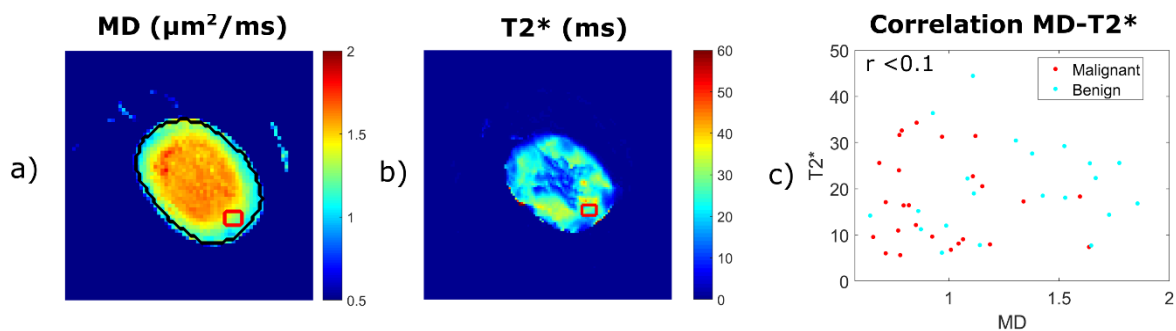
Supporting Information Figure S1 - Flow chart illustrating the number of patients and lymph nodes as well as the exclusion criteria for the ex-vivo (left) and clinical (right) studies.

S3. This section presents the ex-vivo results showing the differentiation between benign and malignant lymph nodes based on the standard Diffusion Tensor model.



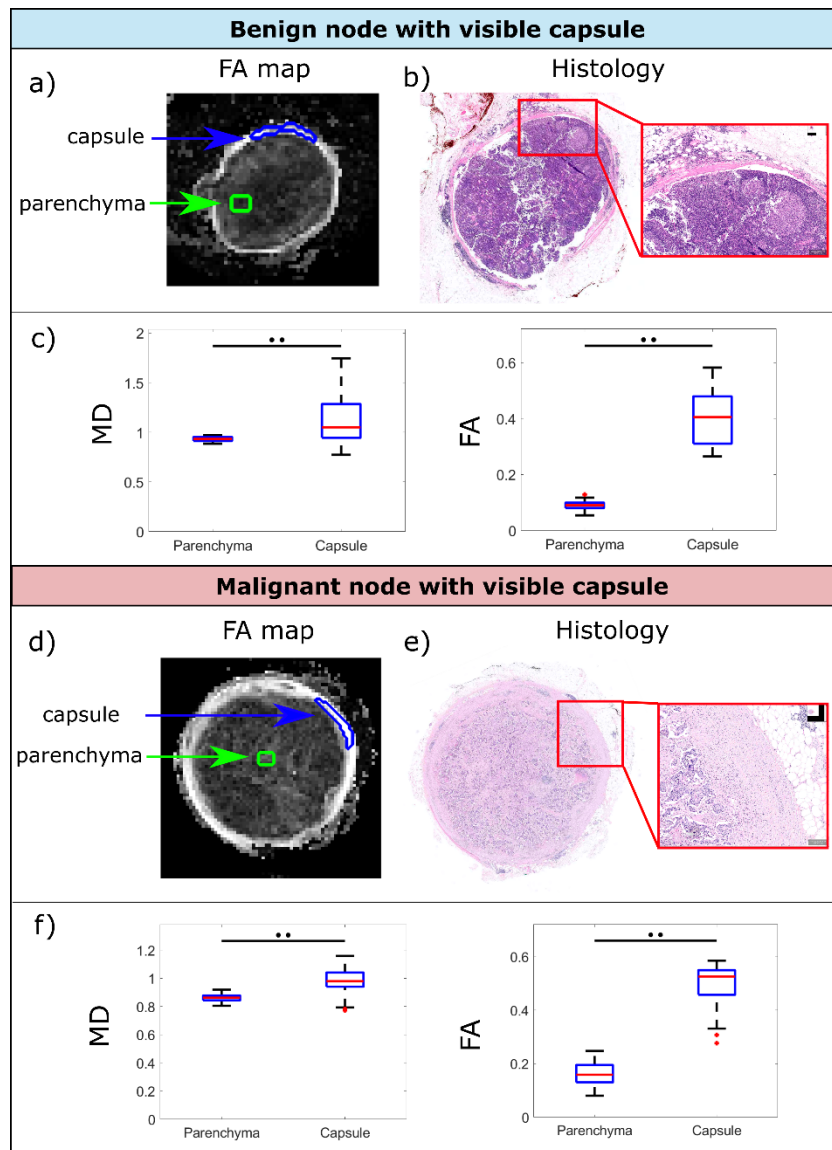
Supporting Information Figure S2 a) Parameter maps derived from the Diffusion Tensor model (MD and FA) for the same benign and malignant lymph nodes presented in Figure 3. b) MD and FA comparison for benign and malignant nodes.

S4. This section presents the correlation between MD from the Ball model and $T2^*$ values calculated from the multi-gradient echo (MGE) data published in (2). To calculate the $T2^*$ values, a mono-exponential function was fitted to the first 10 echoes of the acquisition in (2). For this analysis, similar ROIs to the ones used for the comparison between dMRI data and histology have been drawn on the $T2^*$ dataset, as illustrated in Figure S1 a) and b). Figure S1c) presents the scatter plot between median $T2^*$ and MD values, showing no correlation between the two metrics.



Supporting Information Figure S3 a)-b) Parameter maps of MD and $T2^*$, respectively; c) correlation plot between $T2^*$ and MD.

S5. This section presents a comparison of diffusion parameters between the parenchyma and the capsule of a representative benign and malignant node, where the capsule is highly visible in histology and MRI maps. The capsule tissue exhibits significantly higher MD and FA values compared to the parenchyma ($p < 0.01$) both in the benign and malignant nodes.



Supporting Information Figure S4. Comparison of diffusion parameters in the capsule and parenchyma of a benign (a-c) and a malignant (d-f) node. a), d) FA maps illustrating the capsule and parenchyma ROIs; b), e) Histology images highlighting the stromal organization in the capsule; c), f) Boxplots of MD and FA values. All p values < 0.01 .

References:

1. Alexander DC, Dyrby TB. Diffusion imaging with stimulated echoes: signal models and experiment design. arXiv:1305.7367 2013.
2. Santiago I, Santinha J, Ianus A, et al. Susceptibility perturbation MRI (SPI) maps tumor infiltration into mesorectal lymph nodes. Cancer Res. 2019:canres.3682.2018.